Infrared Physics & Technology 67 (2014) 391–396

Contents lists available at ScienceDirect

Infrared Physics & Technology

journal homepage: www.elsevier.com/locate/infrared

Zero bias PIN photodetector based on gradient band distribution and doping gradient profile

Yang Luo *, Yongqing Huang, Ge Zang, Xiaomin Ren, Xiaofeng Duan, Shiwei Cai, Qi Wang, Xia Zhang, Jun Wang

State Key Laboratory of Information Photonics and Optical Communications, Institute of Information Photonics and Optical Communications, Beijing University of Posts and Telecommunications, Beijing 100876, China

HIGHLIGHTS

- Zero bias photodetector was designed based on doping gradient profile.
- The two aspects of the design of the high-speed low-bias photodetector were explained.
- It can reduce the operation bias and improve the frequency response effectively.
- The best value of the reverse bias for a photodetector was explained.

ARTICLE INFO

Article history:
Received 17 June 2014
Available online 16 September 2014

Keywords:
Zero bias photodetector
Optical fiber communication
Frequency response
Gradient band
Doping gradient profile

ABSTRACT

Zero bias photodetector which was suitable for top-illuminated and side-illuminated was fabricated. Maximal bandwidth-efficiency product (BEP) value could be achieved when the epitaxial layer structure was optimized. The 3-dB bandwidth of the zero bias was 12.27 GHz, which was numerically above 80% of that maximum value. The measured external quantum efficiency of the photodetector was 17% at the zero bias and 1550 nm. The dark current of the photodetector with 12-μm diameter was less than 9×10^{-8} A at a reverse bias of 0.1 V. The influence of doping gradient profile on photodetector performance was illustrated by simulation comparison. The important aspects of the design of the high-speed low-bias photodetector were explained. The phenomenon of the photodetector at the reverse bias which was not the higher the better was explained. The improvement in performance of the photodetector was discussed. The fabrication process and the testing process were described in detail.

Crown Copyright © 2014 Published by Elsevier B.V. All rights reserved.

1. Introduction

The photodetector is the key component in the optical fiber communication system and optoelectronic integration system. The optoelectronic integration system using ultra-low bias, low-loss of sensors and components has become the development trend. Therefore, ultra-low bias, low-loss photodetectors and sensors are an important research topic of the high-speed optoelelctronic integration system. At the same time, the application that the power is transmitted by optical fiber cable instead of the traditional copper line is a new field of the zero bias photodetectors. The low bias photodetectors are the most potential devices which are fabricated by using group III–V materials for optical communication system. Recently, some applications of high performance zero bias photodetectors have been reported in [1–10]. The zero bias photodetector has great significance in optical fiber communication system because it will simplify the installation and eliminate the power circuit.

In this work, we designed and implemented a zero bias PIN photodetector based on gradient band distribution and doping gradient profile. Some zero bias photodetector structures designed by using the gradient band gap in the barrier layer have been reported in [11–21]. It could significantly decrease the operated reverse bias. The p-doped gradient barrier and n-doped gradient depletion layers can smooth the band to improve the frequency response characteristic.

Bandwidth-efficiency product (BEP) was considered to be an indicator to optimize the performance of PIN photodetector. The photodetector had obvious photovoltaic (PV) effect as expected. The 3-dB bandwidth comparative tests were completed under various reverse bias conditions. The 3-dB bandwidth of the photodetector at the zero bias was 12.27 GHz, which was numerically

---

* Corresponding author.

http://dx.doi.org/10.1016/j.infrared.2014.09.008
1350-4495/Crown Copyright © 2014 Published by Elsevier B.V. All rights reserved.

exceeding eighty percent of that at reverse bias of 3.3 V. The external quantum efficiency of the photodetector was 21.14% at 1550 nm wavelength and reverse bias of 3.3 V. It meant that the responsivity was 0.2638 A/W. The dark current of the photodetector was 9×10^{-8} A at the reverse bias of 0.1 V. In the following section, the fabrication process of the zero bias photodetector would be described in detail.

2. Design and fabrication

2.1. Design and optimization

High speed zero bias photodetector was designed by two important reference conditions. A condition was a high built-in electric field in the depletion layer obtains the close to saturation velocity of carriers. Another condition was to use gradient band distribution to reduce the operation bias. To reduce the transit time, it could achieve by decreasing the InGaAs absorption layer. However, the quantum efficiency was sacrificed at the same time. Due to this reason, there must be tradeoff between the transit time and quantum efficiency. So, the bandwidth-efficiency product (BEP) became an effective and convenient indicator to evaluate the performance of photodetector. We changed the thickness of the absorption layer from 100 nm to 1000 nm. The maximal BEP was obtained when the thickness was 350 nm through simulations and calculations. Fig. 1 shows the normalized bandwidth efficiency product with various thicknesses of the absorption layer.

After obtaining the maximal BEP, the detail epitaxial structure was determined as shown in Table 1. The device simulator from Silvaco was used for simulation. The band diagram and electric field distribution which were under 0 V, −1 V, −3.3 V were shown in Fig. 2. The built-in electric field was 16.5 kV/cm at 0 V, 42.8 kV/cm at −1 V, 64 kV/cm at −3.3 V, respectively. The photogenerated carriers velocity was high enough at the zero bias. Its velocity was close to the saturation velocity.

In order to explain the influence of doping gradient profile on the electric field, we designed a uniform doping structure of photodetector following commercial PIN doping profile. Fig. 3(a) shows the detailed epitaxial structure of uniform doping. Fig. 3(b) shows the simulation results of the electric field distribution, which was under 0 V, −1 V, −3.3 V respectively. The electric field intensity of uniform doping profile was smaller than the electric field intensity of doping gradient from Fig. 3(b) (uniform doping: 10.23 kV/cm at 0 V, 25.54 kV/cm at −1 V, 56.26 kV/cm at −3.3 V). And the valence band and conduction band were not significantly smooth. These were unfavorable factors in the frequency response and low bias operation characteristics. The other regions had low electric field. However, the low electric field carriers velocity of InGaAsP and InGaAs is very low which leads to the longer transit time and drop frequency response.

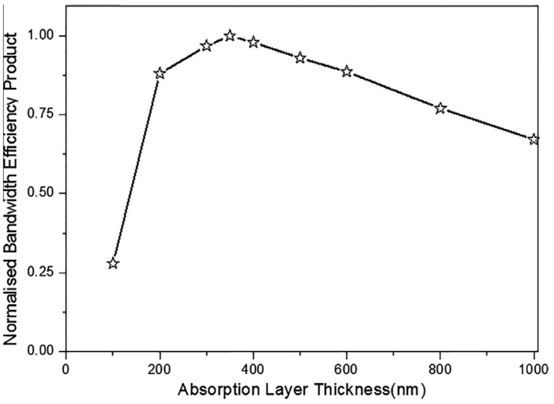

Fig. 1. Normalized bandwidth-efficiency product with various thickness of the absorption layer.

Table 1
Epitaxial structure.

Material	Doping (cm^{-3})	Thickness (nm)
p-InGaAs	p^+ 5×10^{18}	200
p-InP	5×10^{18}	300
p-InP	1×10^{18}	150
p-InP	5×10^{17}	150
p-InP	1×10^{17}	150
p-InGaAsP ($\lambda_g = 1.25$ μm)	1×10^{17}	150
i-InGaAs	1×10^{15}	350
n-InGaAsP ($\lambda_g = 1.25$ μm)	6×10^{16}	150
n-InP	1×10^{17}	100
n-InP	5×10^{17}	100
n-InP	1×10^{18}	120
n-InGaAs	5×10^{18}	10
n-InP	N^+ 5×10^{18}	900

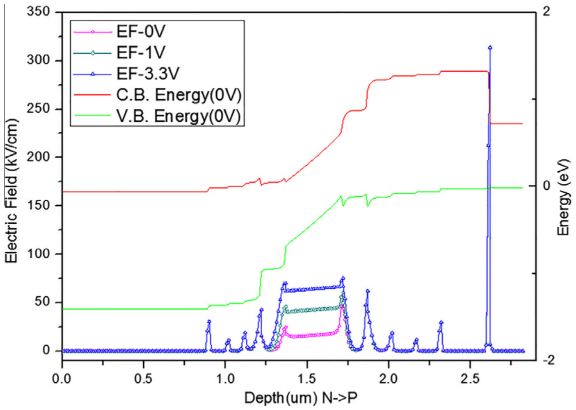

Fig. 2. The band diagram and electric field distribution of doping.

Meanwhile, the frequency response simulation results of the photodetector with different doping profiles and bias were shown in Fig. 4. The diameter of illuminated window was set to 12 μm in simulation environment, so the illuminated window area of the photodetector is 113 μm^2. The simulation light intensity was 250 W/cm^2, so the power of the light is 283 μW, which was consistent with actual small signal measurement power. Under the same conditions, in comparison to uniform doping, the frequency response of doping gradient profile was significantly improved. The bandwidth was 1 GHz, 1.83 GHz, 2.06 GHz, which the uniform doping photodetector was under 0 V, −3.3 V, −10 V respectively. The bandwidth was improved negligibly when the boosted reverse bias was over 10 V. The bandwidth was 13.2 GHz, 19.9 GHz, 7.47 GHz, which the doping gradient photodetector was under 0 V, −3.3 V, −10 V respectively. Bandwidth was significantly brought down, when the reverse bias was over 3.3 V. It means that the frequency response bandwidth of doping gradient photodetector had saturated under lower bias. It also reflects the doping gradient photodetector has a lower bias operation feature.

The figure of normalized frequency response bandwidth was obtained based on the same simulation conditions and variable reverse bias voltage conditions only. We tried to get the saturation bias voltage point by corresponding the highest frequency response bandwidth from the figure. Normalized frequency response bandwidth under various reverse bias voltages is shown in Fig. 5. The maximum value of the frequency response bandwidth was obtained at the reverse bias of 3.3 V. The photodetector biased

Download English Version:

https://daneshyari.com/en/article/1784244

Download Persian Version:

https://daneshyari.com/article/1784244

Daneshyari.com